THE JOURNAL OF PHYSICAL CHEMISTRY Letters

LETTER

pubs.acs.org/JPCL

Atomistic Characterization of Stochastic Cavitation of a Binary Metallic Liquid under Negative Pressure

Qi An,[†] Glenn Garrett,[‡] Konrad Samwer,[‡,§] Yi Liu,[†] Sergey V. Zybin,[†] Sheng-Nian Luo,[∥] Marios D. Demetriou,[‡] William L. Johnson,[*,‡] and William A. Goddard, III[*,†]

[†]Materials and Process Simulation Center and [‡]W. M. Keck Laboratory of Engineering Materials, California Institute of Technology, Pasadena, California 91125, United States

[§]I. Physik Institute, University of Goettingen, Goettingen, Germany

[∥]Los Alamos National Laboratory, Los Alamos, New Mexico 87545, United States

ABSTRACT: We demonstrate the stochastic nature of cavitation in a binary metallic liquid $Cu_{46}Zr_{54}$ during hydrostatic expansion by employing molecular dynamics (MD) simulations using a quantum mechanics (QM)-derived potential. The activation volume is obtained from MD simulations and transition-state theory. Extrapolation of the pressure dependence of the activation volume from our MD simulations to low tensile pressure agrees remarkably with macroscale cavitation experiments. We find that classical nucleation theory can predict the cavitation rate if we incorporate the Tolman length derived from the MD simulations.

SECTION: Statistical Mechanics, Thermodynamics, Medium Effects

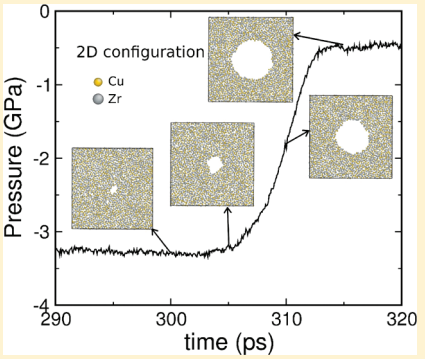

Cavitation or the formation of bubbles in metastable liquids has been investigated experimentally and theoretically since Lord Rayleigh,[1−6] yet there remain considerable uncertainties in the underlying descriptions. Whereas it has been exploited for practical uses including ultrasonic cleaning[7,8] and sonoluminescence,[9] cavitation is directly relevant to undesirable natural events including volcanic eruptions and void formation in solids or glasses that degrade their mechanical, physical, and chemical properties (e.g., fracture, shear banding, and corrosion). In particular, cavitation during isochoric cooling of a metallic liquid may lead to voids at grain boundary triple junctions or randomly dispersed in a metallic glass. This has been difficult to characterize for most metallic glasses because they are normally multicomponent. However, bulk binary metallic glasses have recently been developed (e.g., Ni−Nb and Cu−Zr glasses), thus simplifying the analysis for elucidating the physics underlying cavitation in engineering metallic glasses and alloys.

Cavitation in a metastable liquid is a fluctuation-driven process that is described using classic nucleation theory (CNT).[10−12] However, direct application of CNT to cavitation is complex, considering the closeness of the thermodynamic state to the spinodal and the lack of reliable constraints on such parameters as surface tension. Molecular simulations (molecular dynamics (MD) and Monte Carlo method) and statistical theories have provided some insight into this phenomenon at a more fundamental level.[13−20] However, recent MD simulations of cavitation dynamics in liquids appear to disagree with the cavitation rate from CNT, likely because of uncertainties in estimating the surface tension.[13,14] Recent studies on the fracture of Lennard-Jones liquid evaluated the pressure-dependent surface tension using Tolman model. They estimate the CNT nucleation rate by assuming a constant surface tension leading to disagreement with CNT and MD simulations.[21] To connect MD simulations with transition state and nucleation theories and with experiments, we report MD simulations of cavitation in a binary metallic liquid, $Cu_{46}Zr_{54}$, under negative pressure using a potential function (force field) derived from QM. Our studies show that cavitation can be described as a random Poisson process. Indeed, using the activation volume obtained from the transition-state theory and the surface energy from the Tolman length model, we find that CNT predicts the cavitation rates in accord with direct MD simulations. We characterize the pressure dependence of the activation volume within a limited range of pressure and show that the extrapolation to lower pressures leads to good agreement with experiments.

Our MD simulations use the Rosato−Guillope−Legrand potential[22,23] for Cu−Zr alloy extracted from density functional theory calculations on CuZr compounds and implemented in the ITAP MD program.[24] Previous studies[23,25,26] showed that this potential is accurate: the predicted glass formation temperature (∼700 K), bulk structure, elastic moduli, and viscosity agree with available experiments.

Received: March 15, 2011
Accepted: May 12, 2011
Published: May 12, 2011

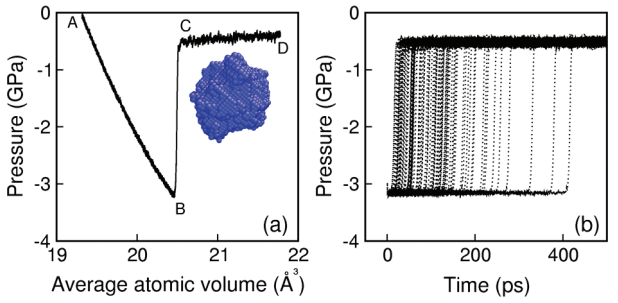

Figure 1. (a) Pressure−volume plot for the 54 000-atom system under hydrostatic tension at 1200 K; inset: an example of the cavity near *C* (∼0.9 nm in radius). (b) Pressure evolutions for 100 independent NVT runs, all started with the same configuration at $P = -3.16$ GPa in part a.

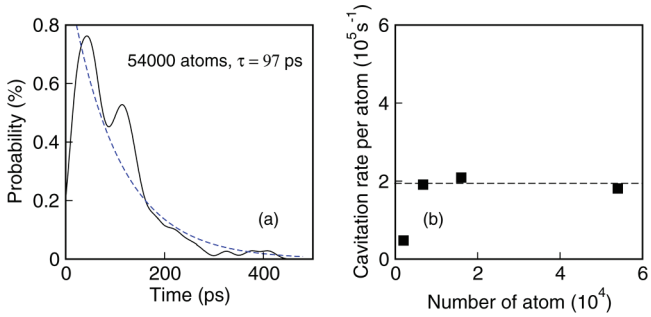

Figure 2. (a) Probability of cavitation obtained from 100 independent runs on the 54 000-atom system (solid line) and Poisson fitting (dashed line). $T = 1200$ K and $P = -3.16$ GPa. (b) Cavitation rates (per atom) for four different system sizes under the same loading conditions.

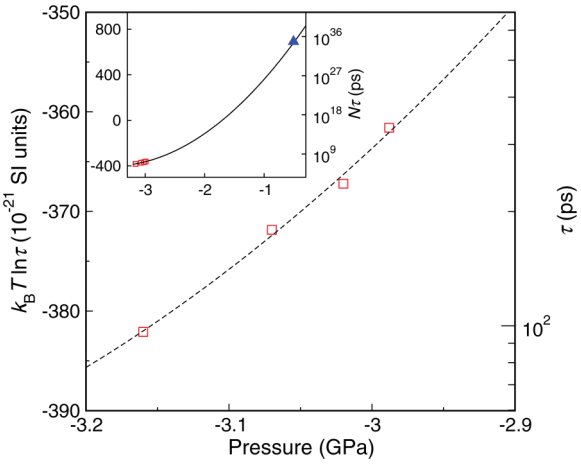

Figure 3. $k_BT \ln \tau$ (left axis) and τ (right axis) as a function of initial pressure P for the 54 000-atom system at 1200 K. MD results: squares; dashed line: quadratic fitting. Inset: Extrapolation of MD results to experimental scales. The experiment point (triangle) has $\tau \approx 7$ s for a system size of 10^{22} atoms.

We first construct binary $Cu_{46}Zr_{54}$ systems with periodic cells ranging from 2000 atoms to 54 000 atoms with random atom positions. Using an integration time step of 1 fs, we melt the systems at 1200 K and equilibrate them for 100 ps for subsequent cavitation simulations. For tensile loading, we expand the cell at a uniform expansion rate of 2×10^8 s^{-1} at 1200 K using a single Nosé−Hoover thermostat (constant volume-temperature or NVT ensemble, with a Nosé−Hoover time constant of 20 fs). Various time constants for thermostats (10∼100 fs) we tested are found to have no effect on simulation results. The strain rate we use enables the liquid to achieve equilibrium before cavitation occurs. To explore the stochastic nature of cavitation, we carried out 100 independent calculations for a given initial, metastable state. In each of these runs, we changed only the initial velocity distributions (via changing the random number seed for velocity assignment) and observe the cavitation dynamics. To calculate the cavity volume within the binary liquids, we use a grid-based void analysis method.[27] Given the cavity volume, we can obtain the cavity radius by assuming that the cavity has a spherical shape.

Figure 1a shows the pressure evolution as a function of volume (or bulk strain) for the 54 000-atom system under tension at a constant strain rate and fixed temperature (T). With increasing strain, pressure (P) decreases steadily (AB) until it reaches the pressure minimum B. AB is the liquid equation of state at fixed temperature, and pressure minimum B is expected to be close to spinodal. There is a drastic decrease in the magnitude of P after B due to tensile stress relaxation accompanying rapid cavity nucleation and growth (BC). The system then reaches a steady state (CD) where P increases slowly. Cavitation during BCD is confirmed by direct analysis, and an example of the cavity is shown as an inset to Figure 1a. The cavity is approximately spherical but with a rugged surface on the MD scale.

To analyze the onset of cavitation of this metastable binary liquid, we follow its evolution under a fixed bulk volume and temperature. We choose various starting configurations from Figure 1a prior to the pressure minimum B to explore homogeneous cavitation under different loading conditions. For each such configuration, we performed NVT simulations (with fixed bulk volume and temperature) and observed the cavitation dynamics under the prescribed tensile loading. The point of cavitation is obvious in the change of the instantaneous bulk pressure. Starting from a specific initial configuration (e.g., near B in Figure 1a), we carried out 100 independent NVT runs; for each run, a different random number seed is used for initial velocity assignment. Figure 1b shows the results from 100 runs all starting at a precavitation loading of $P = -3.16$ GPa. For each run, P remains constant for a while and then increases rapidly as a result of cavity nucleation and growth, finally reaching a plateau in which the stress is in equilibrium (Figure 1b). The pre- and postcavitation values of P are the same for all 100 independent runs. However, cavitation occurs at very different individual waiting times (t_{wait}). Here t_{wait} is the instant at which the pressure amplitude decreases to the midpoint between the pre- and postcavitation values. The exact cavitation time is the point at which the nuclei reach the critical point, which is hard to derive from direct MD simulations. Instead, we define t_{wait}, which is easy to extract. This value is also reliable because the pressure drops fast over the ∼10 ps for initiating the cavitation process.

For a given precavitation pressure, the statistical runs yield 100 values of t_{wait} used to construct the probability distribution (solid line in Figure 2a). Here each point is broadened into a Gaussian of width 15.[28] Fitting the solid line to a Poisson process leads to the dashed line with an expected waiting time $\tau = 97$ ps. The nucleation or cavitation rate follows as $\nu \equiv 1/(N\tau)$, where N is the system size. Here we obtain $\nu = 1.9 \times 10^5$ s^{-1} per atom for the 54 000-atom system at precavitation pressure of −3.16 GPa and 1200 K. To determine whether $N = 54\,000$ is sufficiently large for studying cavity nucleation, we performed similar simulations for

dx.doi.org/10.1021/jz200351m | J. Phys. Chem. Lett. 2011, 2, 1320–1323

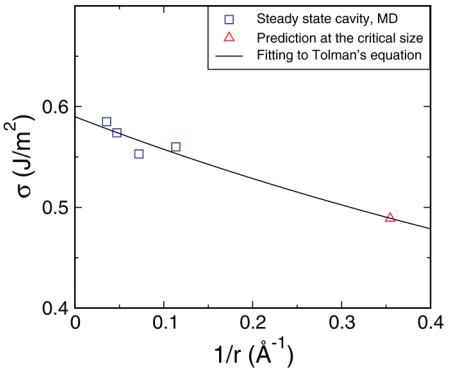

Figure 4. Surface energy σ versus inverse cavity size (r^{-1}).

N = 2000, 6750, and 16 000. Figure 2b shows that ν is similar for three different system sizes with $N \geq 6750$ ($\sim 2\times 10^5$ s^{-1} per atom or 10^{34} s^{-1}m^{-3}), indicating that cavity nucleation is a local phenomenon.

Using transition-state theory, we can write the cavitation rate as $\nu \propto \exp(-\Delta G^{\ominus}/k_B T)$, where k_B is the Boltzmann constant. The Gibbs energy of activation $\Delta G = \Delta\Omega^{\ominus} P - \Delta S^{\ominus} T$ if we neglect the minor composition change near the cavity. The activation volume is $\Delta\Omega^{\ominus} = (\partial \Delta G^{\ominus}/\partial P)|_T$, and the activation entropy is $\Delta S^{\ominus} = -(\partial \Delta G^{\ominus}/\partial T)|_P$. Our simulations are performed at a fixed temperature, so the $\Delta S^{\ominus}$ term can be neglected. From transition-state theory and the definition of ν ($1/N\tau$), we obtain

$$\Delta\Omega^{\ominus} = \left.\frac{\partial (k_B T \ln \tau)}{\partial P}\right|_T \qquad (1)$$

Thus, given τ for various tensile loadings, $\Delta\Omega^{\ominus}$ can be obtained as a function of P. (Similarly, the activation entropy can be obtained via varying temperature at a fixed pressure.) For the 54 000-atom system, we also performed runs at lower tensile loading to obtain longer waiting time τ. Figure 3 shows the plot of $k_B T \ln \tau$ versus P, and its slope is the activation volume. Assuming a linear dependence of activation volume on P, we fit the $k_B T \ln \tau - P$ data points with a quadratic function. This leads to $\Delta\Omega^{\ominus} = 820.7 + 229.3P$ at T = 1200 K, where pressure is in GPa and volume is in Å^3. For a precavitation pressure $P = -3.16$ GPa, the activation volume is 94 Å^3 at 1200 K, corresponding to about five vacancies under ambient conditions.

Cavitation nucleation experiments were carried out on $Zr_{41.2}Cu_{12.5}Ti_{13.8}Be_{22.5}Ni_{10}$ (Vitreloy 1) liquid inside fused quartz ampules of ~0.75 mL volume. Because the liquid has a higher coefficient of thermal expansion, we find that upon quenching below T_g the hot interior liquid cools and shrinks in volume more than the solid shell of fused silica and vetrified liquid that contains it. This results in the buildup of negative hydrostatic pressure in the liquid. Cavities formed within the quenching time scale of 7 s at an estimated temperature of ~1200 K and $P = -0.5$ GPa (triangle, inset to Figure 3) (unpublished results).

To compare with the experiments, we extrapolated the fitted $k_B T \ln \tau - P$ relation to lower pressures, leading to excellent agreement with the experiments (Figure 3 inset). This agreement between the experiments and direct MD simulations lends support to the transition-state theory analysis. Note that the local strain rate and the cavity growth rate in our MD simulations and the loadings are different in the experiments. We find that increased precavitation tensile loading leads to higher growth rates. In Figure 3, the rate effect is implicitly incorporated in the precavitation pressure.

For steady states where a cavity is in equilibrium with the surrounding liquid, the surface energy (σ) is $\sigma = \Delta P/2r$, where ΔP is the pressure difference across the cavity surface and r is the radius of the cavity at steady state. We construct a cavity (radius ~25 Å) within the liquid at 1200 K, vary the bulk volume and let the system achieve equilibrium, and then measure the steady-state cavity size and pressure to calculate the corresponding σ. The results of σ for different cavity sizes are shown in Figure 4 (squares), which can be fitted with the Tolman equation

$$\sigma(r) = \frac{\sigma_0}{1 + \dfrac{2\delta}{r}} \qquad (2)$$

where the Tolman length δ = 0.3 Å and σ_0 = 0.59 J m^{-2} is the surface energy for a planar surface (Figure 4). We apply the Tolman equation to both steady and transient states. For $P = -3.16$ GPa and T = 1200 K, $\Delta\Omega^{\ominus}$ = 94 Å^3 and r = 2.8 Å; the surface energy corresponding to this activation volume is σ = 0.49 J m^{-2} from the Tolman equation (triangle in Figure 4).

In classical nucleation theory, the driving force for cavity nucleation is $\Delta G = 4\pi r^2\sigma + 4/3\pi r^3 P$, where the first (surface) term is the free energy gain due to surface tension of a cavity and the second (volume) term is the reduction while creating the cavity. ΔG peaks at the critical value (ΔG^*) with the critical radius $r^* = 2\sigma/P$, and $\Delta G^* = 16\pi\sigma^3/3P^2$. Our application of CNT assumes an ideal gas with an incompressible liquid and ignores the number of atoms in the bubble. Assuming that the activation volume at $P = -3.16$ GPa and T = 1200 K from transition-state theory is the corresponding critical nucleus size, we obtain a critical radius of r^* = 2.8 Å for use in CNT. From our MD, we obtain σ = 0.49 J m^{-2} from the Tolman equation. This leads to ΔG^* = 1.23 eV.

Given ΔG^* at $P = -3.16$ GPa and T = 1200 K, CNT allows us to estimate the nucleation rate at the critical point: $\nu = \nu_0 \exp\{-\Delta G^*/k_B T\}$. Considering that the cavitation in vitreous liquids is related to the spontaneous and cooperative reorganization of individual clusters near the shear transformation zones (STZs), we believe that the kinetic feature of the liquid is related to the merging of α and β relaxations at high temperatures.[29] Thus, the prefactor ν_0 is related to the Maxwell relaxation time,[30] configurational entropy of critical cavity, and the size of STZs. Therefore, the prefactor is $\nu_0 = (1/N^*)(\mu/\eta) \exp\{n\Delta S/k_B\}$. Here μ is the shear modulus, η is the viscosity, μ/η is the Maxwell relaxation frequency, N^* is the number of atoms in the STZs (~100 atoms as for glass[31]), ΔS is the configurational entropy per atom, and n is the number of atoms occupying the same volume as the critical cavity. From our previous MD study,[26] μ = 2 GPa and η = 0.2 Pa s under similar conditions. We assume that ΔS is ~1k_B, similar to the entropy of fusion according to Richard's rule, and n = 5 as shown above. It follows that ν_0 is ~1.48×10^{10} s^{-1} and ν is ~1×10^5 s^{-1} per atom, which agrees well with our direct MD simulations (2×10^5 s^{-1}). This agreement shows that the cavitation rate can be predicted from CNT with remarkable accuracy if the Tolman length is included.

Our systematic study shows that cavitation in a binary metallic liquid is a random Poisson process and that such complex processes can be well-described by the transition-state theory and classical nucleation theory. We demonstrate the methodology

of obtaining the activation volume (or entropy) indirectly from MD simulations and the transition-state theory and deducing cavitation rate directly from MD simulations. The classical nucleation theory converges with the simulations in describing the cavitation rate if the Tolman length effect is considered. Our results also bear implications to defined broadly nucleation and growth processes.

AUTHOR INFORMATION

Corresponding Author

*E-mail: wlj@caltech.edu (W.L.J.); wag@wag.caltech.edu (W.A.G.).

ACKNOWLEDGMENT

Q.A., W.A.G., G.G., and W.L.J. would like to thank NSF DMR-0520565 Caltech CSEM for support. K.S. is grateful for support by the DFG via the SFB 602 and the Leibniz-Program. S.N.L. is supported by the ASC program at LANL.

REFERENCES

(1) Plesset, M. S.; Prosperetti, A. Bubble Dynamics and Cavitation. *Annu. Rev. Fluid Mech.* **1977**, *9*, 145–185.

(2) Flynn, H. G. Physics of Acoustic Cavitation. *J. Acoust. Soc. Am.* **1959**, *31*, 1582.

(3) Kornfeld, M.; Suvorov, L. On the Destructive Action of Cavitation. *J. Appl. Phys.* **1944**, *15*, 495–506.

(4) Trevena, D. H. *Cavitation and Tension in Liquids*; Hilger: Bristol, England, 1987.

(5) Suslick, K. S.; Mdleleni, M. M.; Ries, J. T. Chemistry Induced by Hydrodynamic Cavitation. *J. Am. Chem. Soc.* **1997**, *119*, 9303–9304.

(6) Classen, J.; Su, C.-K.; Maris, H. J. Observation of Exploding Electron Bubbles in Liquid Helium. *Phys. Rev. Lett.* **1996**, *77*, 2006–2008.

(7) Niemczewski, B. Proposal of a Test Procedure for Ultrasonic Cleaners. *Trans. Inst. Met. Finish* **2003**, *81*, 28–31.

(8) Maisonhaute, E.; Prado, C.; White, P. C.; Compton, R. G. Surface Acoustic Cavitation Understood via Nanosecond Electrochemistry. Part III: Shear Stress in Ultrasonic Cleaning. *Ultrason. Sonochem.* **2002**, *9*, 297–303.

(9) Putterman, S. J. Sonoluminescence: Sound into Light. *Sci. Am.* **1995**, *272*, 33–37.

(10) Gibbs, J. W. *The Scientific Papers of J. Willard Gibbs*; Dover: New York, 1961.

(11) Viisanen, Y.; Strey, R.; Reiss, H. Homogeneous Nucleation Rates for Water. *J. Chem. Phys.* **1993**, *99*, 4680–4692.

(12) Kashchiev, D. On the Relation Between Nucleation Work, Nucleus Size, and Nucleation Rate. *J. Chem. Phys.* **1982**, *76*, 5098–5102.

(13) Bazhirov, T.; Norman, G. E.; Stegailov, V. Cavitation in Liquid Metals under Negative Pressures: Molecular Dynamics Modeling and Simulation. *J. Phys.: Condens. Matter* **2008**, *20*, 114113.

(14) Kinjo, T.; Matsumoto, M. Cavitation Processes and Negative Pressure. *Fluid Phase Equilib.* **1998**, *144*, 343–350.

(15) Knap, J. M. J.; Ortiz, M. Nanovoid Cavitation by Dislocation Emission in Aluminum. *Phys. Rev. Lett.* **2004**, *93*, 165503.

(16) Neimark, A. V.; Vishnyakov, A. The Birth of a Bubble: A Molecular Simulation Study. *J. Chem. Phys.* **2005**, *122*, 054707.

(17) Okumura, H.; Ito, N. Nonequilibrium Molecular Dynamics Simulations of a Bubble. *Phys. Rev. E* **2003**, *67*, 045301.

(18) Punnathanam, S.; Corti, D. S. Work of Cavity Formation Inside a Fluid Using Free- Energy Perturbation Theory. *Phys. Rev. E* **2004**, *69*, 036105.

(19) Shen, V. K.; Debenedetti, P. G. A Kinetic Theory of Homogeneous Bubble Nucleation. *J. Chem. Phys.* **2003**, *118*, 768–783.

(20) Kusaka, I.; Oxtoby, D. W. Identifying Physical Clusters in Vapor Phase Nucleation. *J. Chem. Phys.* **1999**, *110*, 5249–5261.

(21) Kuksin, A.; Norman, G.; Pisarev, V.; Stegailov, V.; Yanilkin, A. Theory and Molecular Dynamics Modeling of Spall Fracture in Liquids. *Phys. Rev. B* **2010**, *82*, 174101.

(22) Rosato, V.; Guillope, M.; Legrand, B. Thermodynamical and Structural Properties of F.C.C. Transition Metals Using a Simple Tight-Binding Model. *Philos. Mag. A* **1989**, *59*, 321–336.

(23) Duan, G.; Xu, D. H.; Zhang, Q.; Zhang, G. Y.; Cagin, T.; Johnson, W. L.; Goddard, W. A., III. Molecular Dynamics Study of the Binary $Cu_{46}Zr_{54}$ Metallic Glass Motivated by Experiments: Glass Formation and Atomic-Level Structure. *Phys. Rev. B* **2005**, *71*, 224208.

(24) Stadler, J.; Mikulla, R.; Trebin, H.-R. IMD: A Software Package for Molecular Dynamics Studies on Parallel Computers. *Int. J. Mod. Phys. C* **1997**, *8*, 1131–1140.

(25) Duan, G.; Lind, M. L.; Demetriou, M. D.; Johnson, W. L.; Goddard, W. A., III.; Cagin, T.; Samwer, K. Strong Configurational Dependence of Elastic Properties for a Binary Model Metallic Glass. *Appl. Phys. Lett.* **2006**, *89*, 151901.

(26) Duan, G. Simulations, Modeling, and Designs of Bulk Metallic Glasses. Ph.D. Thesis, California Institute of Technology, 2008.

(27) Strachan, A.; Cagin, T.; Goddard, W. A., III. Critical Behavior in Spallation Failure of Metals. *Phys. Rev. B* **2001**, *63*, 060103.

(28) Jones, M. C.; Marron, J. S.; Sheather, S. J. A Brief Survey of Bandwidth Selection for Density Estimation. *J. Am. Stat. Assoc.* **1996**, *91*, 401–407.

(29) Hachenberg, J.; Bedorf, D.; Samwer, K.; Richert, R.; Kahl, A.; Demetriou, M. D.; Johnson, W. L. Merging of the α and β Relaxations and Aging via the Johari-Goldstein Modes in Rapidly Quenched Metallic Glasses. *Appl. Phys. Lett.* **2008**, *92*, 131911.

(30) Masuhr, A.; T.T. Waniuk, R.; Johnson, W. L. Time Scales for Viscous Flow, Atomic Transport, and Crystallization in the Liquid and Supercooled Liquid States of $Zr_{41.2}Ti_{13.8}Ni_{10.0}Be_{22.5}$. *Phys. Rev. Lett.* **1999**, *82*, 2290–2293.

(31) Johnson, W. L.; Samwer, K. A Universal Criterion for Plastic Yielding of Metallic Glasses with a $(T/T_g)^{2/3}$ Temperature Dependence. *Phys. Rev. Lett.* **2005**, *95*, 195501.